

**Fabrication and optical nonlinearities of composite films derived from the water-soluble Keplerate-type polyoxometalate and the chloroform-soluble porphyrin**

Zonghai Shi,<sup>a</sup> Yunshan Zhou,<sup>\*a,b</sup> Lijuan Zhang,<sup>\*a</sup> Di Yang,<sup>a</sup> Cuncun Mu,<sup>a</sup> Haizhou Ren<sup>a</sup>,  
Farooq Khurum Shehzad<sup>a</sup> and Jiaqi Li<sup>a</sup>

<sup>a</sup>State Key Laboratory of Chemical Resource Engineering, Institute of Science, Beijing  
University of Chemical Technology, Beijing 100029, P. R. China

<sup>b</sup>Laboratory of Optical Physics, Institute of Physics, Chinese Academy of Sciences,  
Beijing 100190, P. R. China

**Preparation of the Keplerate-type POM**

$(\text{NH}_4)_{42}[\text{Mo}_{132}\text{O}_{372}(\text{CH}_3\text{COO})_{30}(\text{H}_2\text{O})_{72}] \cdot \text{ca.}300\text{H}_2\text{O} \cdot \text{ca.}10\text{CH}_3\text{COONH}_4$  (denoted  $(\text{NH}_4)_{42}\{\text{Mo}_{132}\}$ ) was prepared according to the literature method [1]. IR ( $\nu/\text{cm}^{-1}$ , KBr): 3424 (s), 1622 (m) ( $\delta(\text{H}_2\text{O})$ ), 1546(m) ( $\nu_{\text{as}}(\text{COO})$ ), 1440 (sh) and 1403 (m) ( $\delta(\text{CH}_3)$ ,  $\nu_{\text{s}}(\text{COO})$ ,  $\delta_{\text{as}}(\text{NH}_4^+)$ ), 969 (m), 945(w-m) ( $\nu(\text{Mo}=\text{O})$ ), 855 (m), 792 (s), 723 (s), 629 (w), 568 (s) (Fig. S1). (The  $\nu$  and  $\delta$ ,  $\gamma$  denote stretching and in-plane bending modes, respectively. The subscripts s and as represent the symmetric and asymmetric modes, respectively). UV-vis. spectrum ( $\lambda/\text{nm}$ ,  $5.5 \times 10^{-7}$  M, in  $\text{H}_2\text{O}$ ): 457, 232 (Fig. S2).

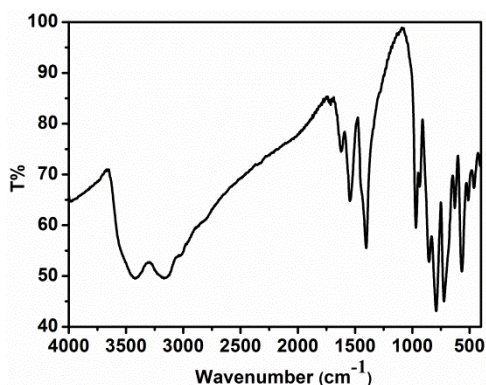


Fig. S1. IR spectrum of the compound  $(\text{NH}_4)_{42}\{\text{Mo}_{132}\}$ .

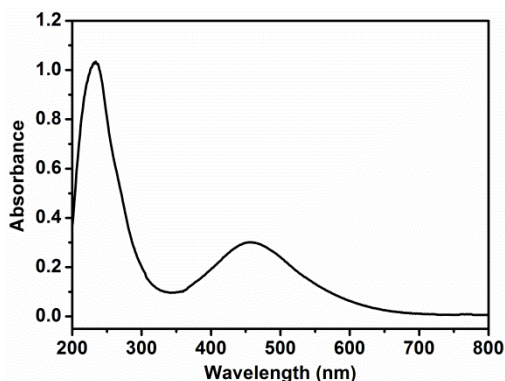


Fig. S2. UV-Vis. spectrum of an aqueous solution ( $5.5 \times 10^{-7}$  M) of the compound  $(\text{NH}_4)_{42}\{\text{Mo}_{132}\}$ .

### Preparation of $[\text{H}_2\text{TPP}](\text{ClO}_4)_2$

$[\text{H}_2\text{TPP}](\text{ClO}_4)_2$  were prepared according to the literature method [2]. IR ( $\nu/\text{cm}^{-1}$ , KBr): 3097 (w) and 3079 (w) ( $\nu_s(\text{C-H})$ ); 3060 (w), 3047 (w) and 3029 (w) (phenyl); 1483 (s) ( $\nu_s(\text{C-C})$ ); 1438 (m) (phenyl); 1232 (m) ( $\delta_{\text{as}}(\text{C-H})$ ); 1211 (w) ( $\delta(\text{N-H})$ ); 1182 (w) (phenyl); 1086 (s) (phenyl +  $\delta_s(\text{C-H})$ ); 1034 (s) (phenyl); 999 (m) ( $\nu_s(\text{pyrrole half-ring})$  + phenyl); 983 (m) and 925 (m) ( $\delta(\text{pyrrole breath})$ ); 909 (m) ( $\delta_{\text{as}}(\text{C-H})$ ); 879 (s) ( $\delta_s(\text{pyrrole def})$ ); 830 (s) ( $\delta_{\text{as}}(\text{pyrrole def})$ ); 811 (s) and 760 (s) (pyrrole fold); 705 (s) ( $\gamma_s(\text{C-H})$  + phenyl); 624 (s) (phenyl) (Fig. S3) (The  $\nu$ ,  $\delta$ ,  $\gamma$  denote stretching, in-plane bending and out-of-plane bending modes, respectively. The subscripts s and as represent the symmetric and asymmetric modes, respectively). UV-vis. spectrum ( $\lambda/\text{nm}$ ,  $4.4 \times 10^{-6}$  M, in DMF): 416, 512, 507, 589, 645 (Fig. S4).

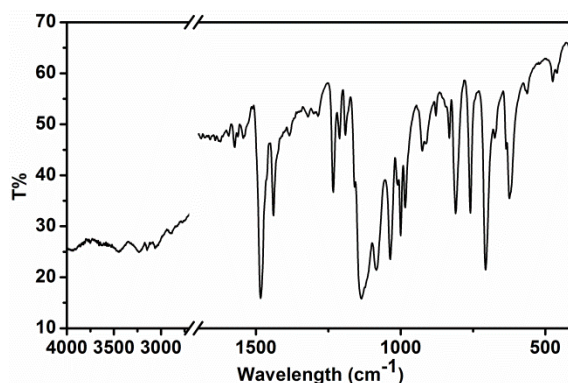


Fig. S3. IR spectrum of the compound  $[\text{H}_2\text{TPP}](\text{ClO}_4)_2$ .

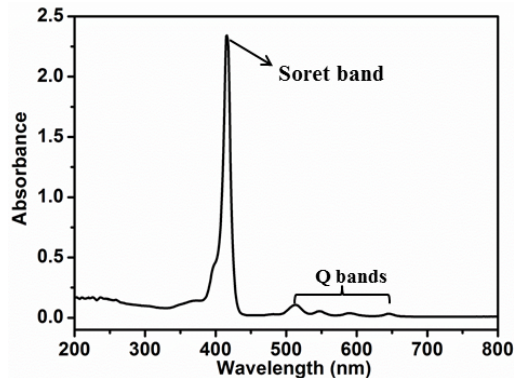


Fig. S4. UV-vis. spectrum of the compound  $[\text{H}_2\text{TPP}](\text{ClO}_4)_2$  ( $4.4 \times 10^{-6}$  M, in DMF)

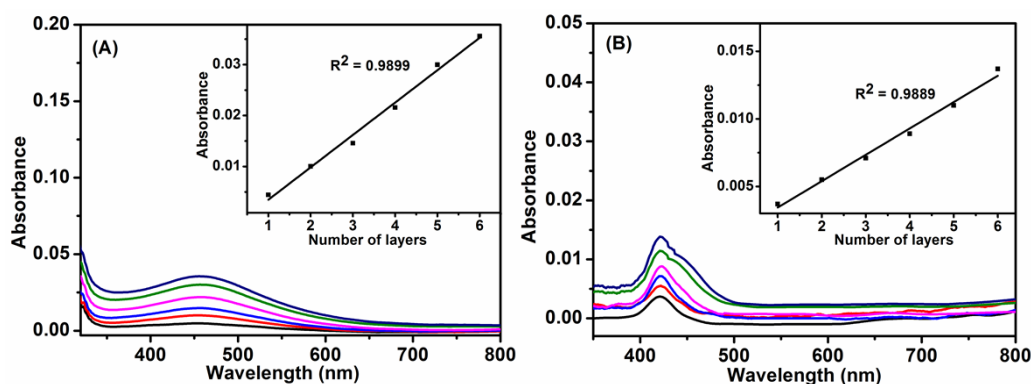


Fig. S5. UV-vis. spectra of  $(\text{PAH}/\{\text{Mo}_{132}\})_n$  ( $n = 0 \sim 6$ ) (A) and  $(\text{H}_2\text{TPP}/\text{PSS})_n$  ( $n = 0 \sim 6$ ) (B) depositing on a quartz substrate. The insets show absorbance at 458 nm and 421 nm versus the layer number of  $(\text{PAH}/\{\text{Mo}_{132}\})_n$  and  $(\text{H}_2\text{TPP}/\text{PSS})_n$  layers, respectively.

The growth process of  $(\text{PAH}/\{\text{Mo}_{132}\})_n$  and  $(\text{H}_2\text{TPP}/\text{PSS})_n$  can be monitored by UV-vis. spectroscopy (Fig. S5). Fig. S5 shows the UV-vis. spectra of the films  $(\text{PAH}/\{\text{Mo}_{132}\})_n$  ( $n = 1 \sim 6$ ) and  $(\text{H}_2\text{TPP}/\text{PSS})_n$  ( $n = 1 \sim 6$ ) assembled quartz substrates. The spectra exhibit the characteristic absorption bands at 458 nm and 421 nm for  $\{\text{Mo}_{132}\}$  and  $[\text{H}_2\text{TPP}]^{2+}$  respectively, which confirms the incorporation of  $\{\text{Mo}_{132}\}$  and  $[\text{H}_2\text{TPP}]^{2+}$  into the multilayers films without any structural alteration, respectively [1, 3]. The band at 445 nm is the characteristic absorption band of  $\{\text{Mo}_{132}\}$  [1]. The band at 421 nm is attributed to Soret band of  $[\text{H}_2\text{TPP}]^{2+}$ . The Q bands of porphyrin are too weak to appear in the spectrum. The polycation PAH and polyanion PSS shows no absorbance above 200 nm, and their presence in the films does not contribute to the UV-vis. spectra. Importantly, as shown in the insets of Fig. S5, the absorbance at 458 nm and 421 nm

versus the layer number of (PAH/{Mo<sub>132</sub>})<sub>n</sub> and (H<sub>2</sub>TPP/PSS)<sub>n</sub> result in two nearly straight lines, which confirm that the {Mo<sub>132</sub>} anions and [H<sub>2</sub>TPP]<sup>2+</sup> cations are smoothly incorporated into the multilayers (PAH/{Mo<sub>132</sub>})<sub>n</sub> and (H<sub>2</sub>TPP/PSS)<sub>n</sub>, respectively.

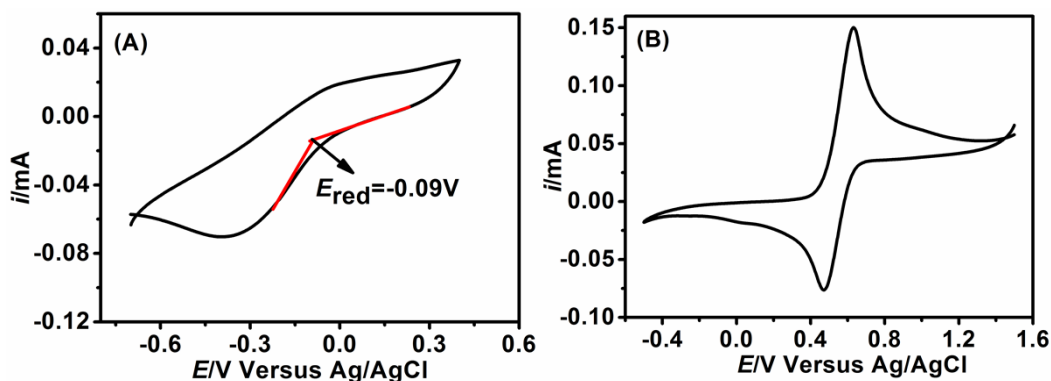


Fig. S6. CV spectra of (NH<sub>4</sub>)<sub>42</sub>{Mo<sub>132</sub>} (in water, 1 mmol·L<sup>-1</sup>, containing 0.5 M CH<sub>3</sub>COOH as a supporting electrolyte) (A), and ferrocene (in DMF, 1 mmol·L<sup>-1</sup>, containing 0.1 M [(n-butyl)<sub>4</sub>N]PF<sub>6</sub> as a supporting electrolyte) (B).

### Calculation of LUMO and HOMO levels of the compound (NH<sub>4</sub>)<sub>42</sub>{Mo<sub>132</sub>}

The molecular orbital levels of (NH<sub>4</sub>)<sub>42</sub>{Mo<sub>132</sub>} were calculated by cyclic voltammetry (CV) spectra (Fig. S6) [4, 5]. The lowest unoccupied molecular orbital (LUMO) level was obtained by  $E_{\text{LUMO}} \text{ (eV)} = -e (4.8 - E_{\text{FOC}} + E_{\text{red}})$  ( $E_{\text{FOC}} = (E_{\text{ox}} + E_{\text{red}})/2$  is energy level of ferrocene used as standard,  $E_{\text{red}}$  is the onset of reduction potential of (NH<sub>4</sub>)<sub>42</sub>{Mo<sub>132</sub>}). The highest occupied molecular orbital (HOMO) level was obtained by  $E_{\text{HOMO}} \text{ (eV)} = E_{\text{LUMO}} - E_{\text{g}}$  ( $E_{\text{g}}$  is the HOMO-LUMO gap of (NH<sub>4</sub>)<sub>42</sub>{Mo<sub>132</sub>} obtained from UV-vis. spectrum by formula  $E_{\text{g}} = 1240/\lambda$  ( $\lambda$  is absorption edge, Fig. S2) [4, 5]. The scan range of the CV were selected carefully from the wide range (+2.5 V ~ -2.5 V) to small range (present in the paper) to insure the peak used for calculating the LUMO level is the onset peak.

### References

- [1] A. Müller, E. Krickemeyer, H. Bögge, M. Schmidtman and F. Peters, *Angew. Chem. Int. Ed.*, 1998; **37**, 3360.

- [2] Z. H. Shi, Y. S. Zhou, L. J. Zhang, C. C. Mu, H. Z. Ren, S. Hassan, D. Yang and H. M. Asif, *RSC Adv.*, 2014, **4**, 50277.
- [3] M. Meot-Ner and A. D. Adler, *J. Am. Chem. Soc.*, 1975, **97**, 5107.
- [4] X. B. Sun, Y. Q. Liu, S. Y. Chen, W. F. Qiu, Y. Gui, Y. Q. Ma, T. Qi, H. J. Zhang, X. J. Xu and D. B. Zhu, *Adv. Funct. Mater.* 2006, **16**, 917.
- [5] B. R. Hyun, Y. W. Zhong, A. C. Bartnik, L. F. Sun, H. D. Abrun, F. W. Wise, J. D. Goodreau, J. R. Matthews, T. M. Leslie and N. F. Borrelli, *ACS Nano*, 2008, **2**, 2206.